

Magnetic Properties and Structure of Cobalt-Hardened Gold

David Kahn
AMP Incorporated

ABSTRACT

The implementation of an experimental design to investigate the variation in cobalt-hardened gold electrodeposition produced a series of electrodeposited AuCo alloys which had been stripped from their copper substrates. The magnetic properties of these electroplating were measured at room temperature using the Faraday method. These measurements showed the presence of two magnetic phases. One phase consisted of a solid solution of cobalt in the gold matrix and the second was found to be a diamagnetic cobalt-containing component. The magnetic measurements showed that no precipitates of metallic cobalt were present and that individual atoms and nearest neighbor pairs of cobalt atoms in the solid solution are not magnetic. The diamagnetic phase cannot contain cobalt hexacyanocobaltate $\text{Co}_3[\text{Co}(\text{CN})_6]_2$, which is found after treatment of the alloy with aqua regia. Also, the second phase cannot all be potassium hexacyanocobaltate $\text{K}_3[\text{Co}(\text{CN})_6]$. Subsequent to these measurements, the platings were annealed in hydrogen at 800°C to destroy any cobalt compounds in the platings, and the magnetic properties were remeasured. These second measurements revealed the existence of only one phase, again a solid solution of cobalt in gold. This phase showed superparamagnetic behavior with some remanence and is a magnetic nanocomposite. The amount of the cobalt in the metallic and compound phase is calculated from the contribution of each phase to the initial slope of the magnetization curve.

INTRODUCTION

The use of gold plating containing small amounts of cobalt [0.3 wt% (1.0 at %)] on electrical contact members is quite common in the electronics industry. Recently the variation in plating efficiency with plating conditions was studied using an experimental design encompassing ten plating bath parameters. One result of this effort was 64 AuCo platings produced in four experimental blocks. These platings were stripped from their copper substrate and their magnetic properties were measured. Since cobalt is a ferromagnetic element and the gold matrix is very weakly diamagnetic, the behavior of the cobalt in the gold alloy should affect the magnetic properties of the samples.

Some of the graphs in this work are presented in the form of the variation of one dependent response on the cobalt content for a number of different samples, although these experiments are not the usual kind where only one independent variable is changed and the others kept constant. Ten plating-bath variables are determined *a priori* for each run, and their values are one of two levels determined by the experimental design. One of these parameters was the cobalt concentration in the bath. Because of this, the dependence of any measured response on the cobalt content is valid only to the extent that the values of the other variables do not affect the magnetic behavior of the cobalt deposited in the electroplated gold alloy. The measurements of the magnetic behavior of a single sample are not affected by this problem, but this difficulty will arise when the result for one sample is compared to the results for others.

© Copyright 2004 by Tyco Electronics Corporation. All rights reserved.

To determine the total cobalt content, a portion of the stripped AuCo platings were annealed in hydrogen at 800°C to destroy any compound phase that might be present in the alloy plating and furnace cooled.¹ In this report the word organic is used to identify any second phase in the AuCo sample, although as discussed below this phase contains the cobalt in a hexacyanocobaltate salt. The magnetic properties of these annealed samples were also determined. We would expect that these samples are uniform except for the cobalt content, since this treatment probably results in a single metallic phase in the plating. When these annealed platings are dissolved in aqua regia, only a very small amount of black powder remains, which is probably some carbon residue in the plating.

EXPERIMENTAL METHOD

The magnetic susceptibility of the samples was measured at room temperature using the Faraday method. The magnetic field in these experiments was created by a 12-inch electromagnet (Varian Model V-3900) fitted with specially designed (Faraday) pole caps to produce a nearly constant value of $H\partial H/\partial z$ of 14.964 kOe²/cm over a vertical distance of 1.8 cm at a magnet current of 168 A. A gold-plated pure-copper bucket was suspended at this point from a Perkin Elmer AD2B microbalance using a silica optical fiber. The extra force on the sample caused by its magnetization is

$$\delta F_z = m \chi_g H \partial H / \partial z, \quad (1)$$

where m is the mass, and χ_g is the magnetic susceptibility per gram. A schematic of the experimental setup is shown in Figure 1. The samples used were approximately 20 mg and were weighed using a Mettler Type H 15 balance. Since we wanted to measure the magnetic susceptibility over a range of magnetic fields and the pole pieces were calibrated for only one value of the current, the apparatus was calibrated for other values of the current by using a sample of known magnetic susceptibility, cobalt tetrathiocyanatomercurate from SPEX Industries. This calibration was checked by measuring the magnetic susceptibility of a pure gold sample. The magnetic field at intermediate values was measured using the Hall-effect monitor furnished with the magnet control system.

To check the accuracy of the susceptibility measurements, the saturation magnetization of sample III 8 B Annealed was measured for both directions of the field. Results are shown in Figure 2. An extrapolation of the magnetization to an infinite applied field value, for the two results agreed to within 0.16 percent. These measurements show that the observed variation in the magnetic behavior from sample to sample is not due to errors in the magnetic measurements, but is due to real variation in the samples.

EXPERIMENTAL RESULTS

As a result of the limited volatility of cobalt in gold, if the concentration of the cobalt is large enough, some of the cobalt would precipitate into small particles. The Au/Co

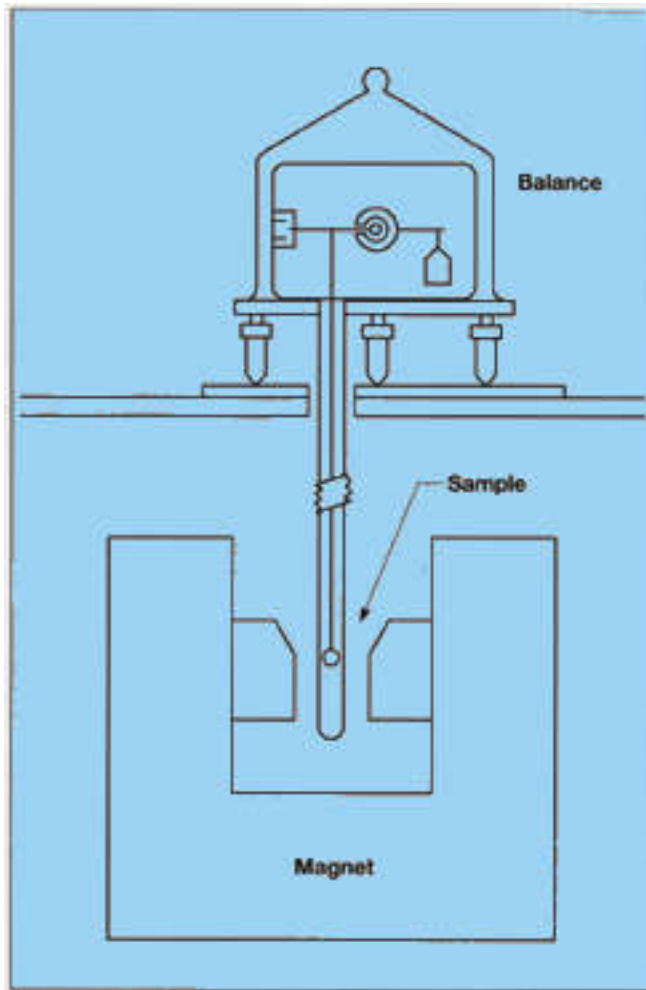


Figure 1. Simple magnetic susceptibility instrument.

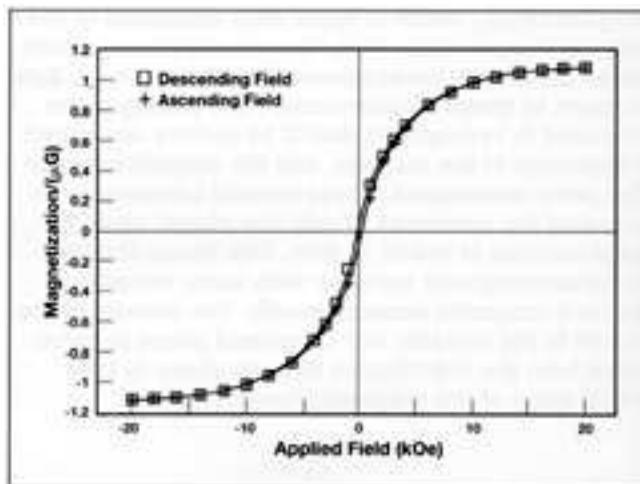


Figure 2. Magnetization versus applied field for an Annealed AuCo Plating.

phase diagram is shown in Figure 3.2 The diagram shows that the volatility of gold in cobalt at room temperature is very low so that any cobalt that might precipitate would be almost pure cobalt and show a corresponding magnetic behavior.

Since cobalt is ferromagnetic with a saturation magnetization, M_s , of 1398 G³ and gold is weakly diamagnetic with a magnetic susceptibility per gram (χ_g) of -1.42×10^{-7} CGS-EMU⁴, any precipitated cobalt will produce a very noticeable magnetic effect. The magnetization of 2 wt% cobalt in a cast CuCo alloy is shown in Figure 4.⁵ In this case the, magnetization is on the order of 10 G for an applied field of 3000 Oe, even though the cobalt particles are small enough to be superparamagnetic. In all of our samples, on the other hand, the magnetization is less than 1.0 mG. Clearly, cobalt precipitates of any reasonable amount cannot be present.

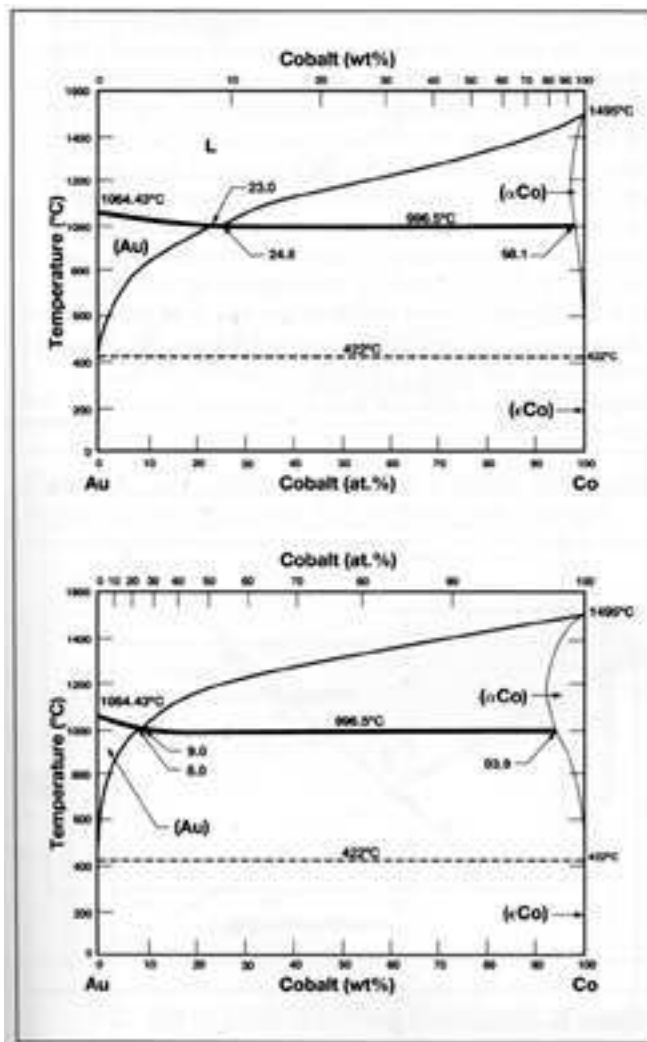


Figure 3. Phase Diagram of the Au-Co System. The triangular areas (Au, α Co) at each end of the diagrams show the maximum amount of one component that can be dissolved in the other at *equilibrium*.

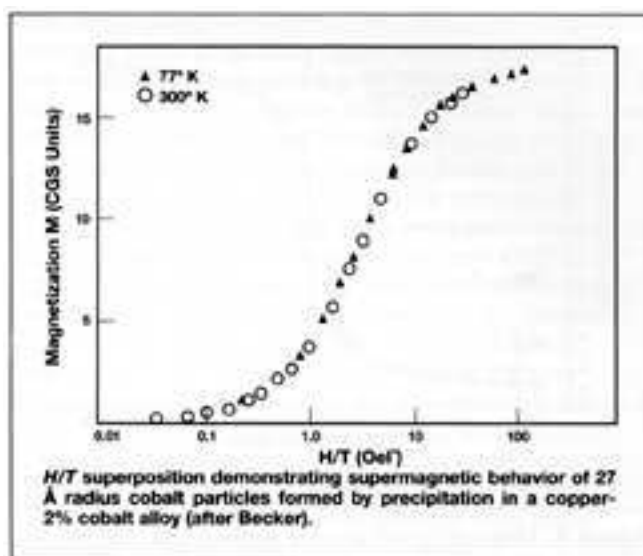


Figure 4. Magnetization versus applied field for cobalt particles precipitated from a copper matrix. The shape of the magnetization curve is different because the logarithm of the applied field is plotted.

In several instances AuCo platings that contained the most cobalt (as determined by magnetic susceptibility measurements) were examined using x-ray diffraction to see if any crystalline cobalt could be detected. Although x-ray diffraction probably is sensitive enough to detect a fraction of a percent of metallic cobalt, no cobalt peaks were seen.

Annealed Platings

A portion of the thick cobalt plating was stripped from the copper substrate, annealed in hydrogen at 800°C for two hours, and furnace-cooled. Magnetization curves for all annealed samples are similar. Magnetization curves for samples with the largest (III 8 B) and the smallest (IV 5 B) cobalt content are shown in Figures 2 and 5.

If each cobalt atom in the alloy retained its magnetic character and the magnetic moments were acting independently, we would expect a paramagnetic behavior of the alloy. The magnetization at room temperature would be a straight line with a positive slope. We see quite a different behavior in our samples, however. The applied field of 20 kOe is large enough to align almost all the available cobalt spins so that the magnetization of the alloy is nearly saturated. This can only mean cooperative interaction between the cobalt spins in the sample. We also notice that there is a small remanence, or residual magnetization, when the applied field is reduced to zero after saturation. The coercive field-the field in the opposite direction required to reduce the remanence to zero-for sample III 8 B is about 130 Oe and the coercive field for sample IV 5 B is close to 1 kOe. A portion of this hysteresis is probably due to some iron impurity and is discussed in more detail below, but the majority is real.

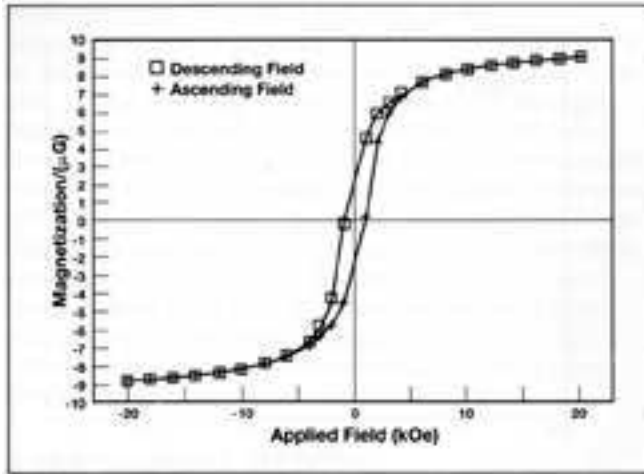


Figure 5. Magnetization versus applied field for an annealed AuCo plating.

The saturation of the magnetization curve would imply the presence of spontaneous magnetization in the alloy, and the existence of a measurable remanence would imply that there is some metastable magnetic behavior. These two results can be explained if almost all the magnetic units are small enough so that they contain only one domain and, in addition, some of these domains are large enough so that the energy of thermal agitation at room temperature is too small to reverse the spin direction because of magnetocrystalline anisotropy.⁶ These domains will not become disordered in the time required to make the magnetic measurement and some remanence will be seen.

Since this measurement is made at a known temperature (22–25°C), if we know the magnetocrystalline anisotropy, K_1 , we can say something about the size of the magnetic entities. The demagnetizing effects of thermal disorder have been calculated by Neel, who derived an upper limit for the volume, V , of a particle that should show saturation but no remanence.⁷ Since a particle with a single domain can change its direction of magnetization only by changing the direction of its moment, this shift will occur fast enough so that no remanence is observed if the energy barrier due to the magnetocrystalline anisotropy is less than about 20 times the thermal energy. In this case the inequality

$$K_1 V / kT < 20 \quad (2)$$

must be satisfied for this type of superparamagnetic behavior. Since the cobalt atoms in the alloy have a cubic symmetry, the usual anisotropy value for hexagonal cobalt does not seem appropriate. Extrapolating the measured value of K_1 for cubic cobalt to room temperature yields a value of approximately -5×10^5 ergs/cm³.⁸ Using this value we find that the upper limit for the diameter of a superparamagnetic entity at room temperature in the gold is 146 Å. Of course, we are assuming here that the anisotropy constant for pure cobalt is still valid for the cobalt in solid solution in gold.

Since we know the amount of cobalt in our samples, we can compare our measured saturation magnetization with that calculated on the assumption that each cobalt atom has the same magnetic moment that it has in pure cobalt ($1.716 \mu_B$).⁹ The calculated value for the saturation magnetization of sample III 8 B Annealed, assuming that each cobalt atom retains its moment, is 48.49 G. Since our measured value is only 1.22 mG, we see immediately that the cobalt in the annealed plating cannot be in the form of a cobalt precipitate. Since the cobalt must then be in solid solution in the gold alloy, we can also conclude that most of the cobalt dissolved in the gold matrix is also not magnetic. If these hypotheses are true, our next question must be, what is then giving rise to the measured magnetism?

Additional information about the distribution of the cobalt atoms in the annealed platings can be obtained by comparing the initial slope of the magnetization curve of each sample with the cobalt concentration in the sample. Figure 6 shows the data for Block II. This figure is especially interesting in that the cobalt concentration in the plating bath is only one of two values for each sample. The regression of the initial slope on the cobalt concentration shows that the slope increases almost as the third power of the concentration. The reason is that superparamagnetism is a cooperative phenomenon and the contribution from any cobalt atom in solution depends on how many cobalt atoms are nearby. This effect has been investigated by Boucai *et al.*, who found that isolated cobalt atoms in a gold matrix are not magnetic, isolated pairs are also not magnetic at room temperature, but groups of three or more atoms have a magnetic moment and can lead to magnetic ordering at low temperatures.¹⁰

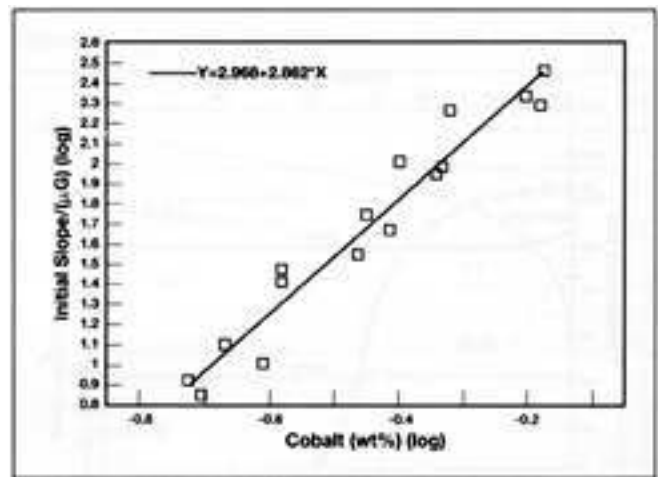


Figure 6. Variation in the initial slope of the magnetization versus applied field curve with total cobalt concentration.

Figure 7 shows a plot of data taken from Reference 10 of the variation with cobalt content of the calculated probabili-

pairs of cobalt atoms (N_2/N), cobalt atoms in groups of three (N_3/N), and all larger groups (N_4/N). We can see clearly that the probability of finding a group of three, or more, cobalt atoms is very small for low concentrations of dissolved cobalt and becomes appreciable only for concentrations larger than approximately 0.2 wt% cobalt. The total cobalt concentrations in the platings made for this study vary from 0.1495 to 0.691 wt%, The probability per lattice site of the sum of N_3/N and N_4/N is plotted in Figure 8. Here we see that the sum varies as the 2.902th power of the cobalt concentration. This is very close to the behavior shown in Figure 6, which shows a very similar dependence on the cobalt concentration. Similar plots for the other blocks show the same concentration dependence.

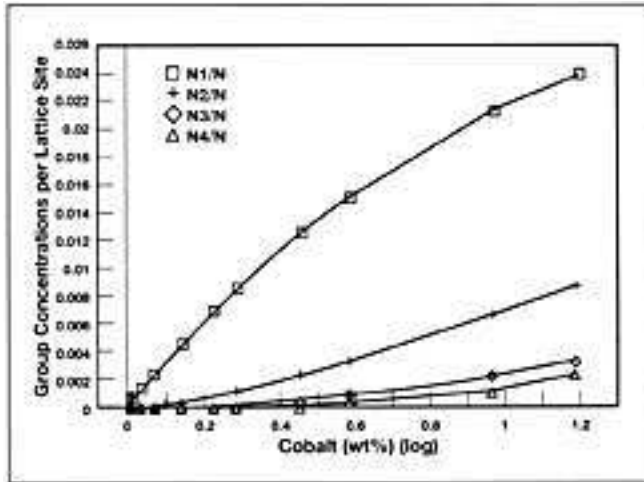


Figure 7. Calculated probability of a cobalt site having zero (N_1), one (N_2), two (N_3) or more (N_4) nearest.

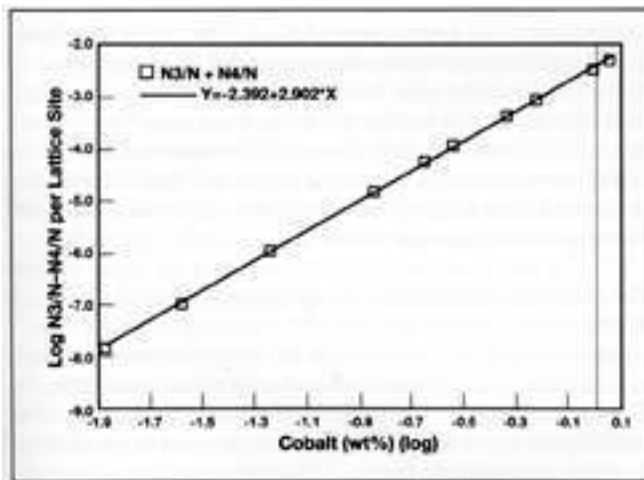


Figure 8. Calculated probability of a cobalt site having two or more nearest neighbor cobalt atoms versus cobalt concentration.

The nonmagnetic behavior of single atoms and close pairs of cobalt atoms in the alloy cannot explain the total reduction in alloy magnetization that we measure in sample III 8 B Annealed. From Reference 10 the number of cobalt atoms in a mole of alloy included into isolated groups of three or more nearest neighbor cobalt atoms is just the sum of N_3 and N_4 . This number for sample 1118 B Annealed (0.68 wt%) is $1.322 \times 10^{-3}N$, where N is Avogadro's number. In a gram of sample III 8 B Annealed, we have 4.043×10^{18} cobalt atoms that are magnetic. The ratio of the measured saturation magnetization for this sample to the calculated magnetization if all cobalt atoms carry their metallic "moment is 1.32×10^{-4} . This means that the magnetic moment of the cobalt atoms in the alloy that are magnetic is approximately $0.0023 \mu_B$. This shielding of the impurity atom is not too surprising since the Kondo temperature for isolated cobalt gold atoms in gold has been estimated to be 500 K (226.8°C). Below this temperature we expect a shielding of the impurity magnetic moment.¹¹

The results discussed above are clearly consistent with an annealed alloy plating containing a random solid solution of cobalt in a gold matrix. The amount of cobalt in these platings has been measured using an inductively coupled plasma emission spectrometer and has been denoted as total cobalt.

Unannealed Platings

The unannealed platings show a different magnetic behavior. In most of the platings, a plot of the magnetization versus applied field is similar to the one for 1118 B Unannealed in Figure 9. We can see here that the magnetization shows a behavior that is a combination of ferromagnetic and paramagnetic behavior with clear evidence of some saturation but no apparent hysteresis and a magnetization that is on the order of 10 mG. Since the Langevin function at high field values varies as $1 - kT/mH$, if we plot the magnetization versus $1/H$, we can extrapolate the points at large fields to find

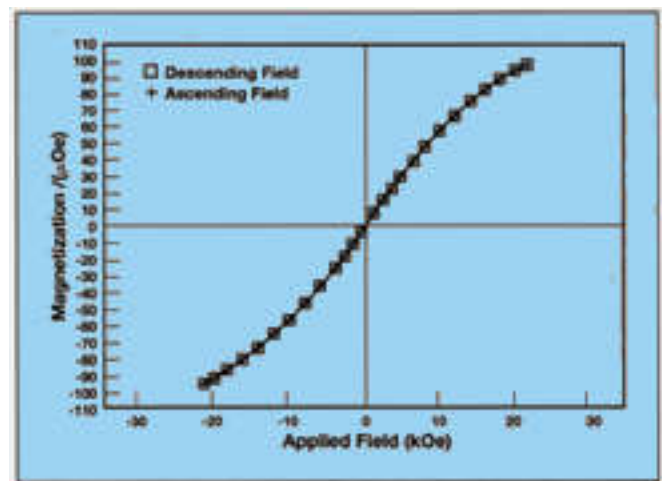


Figure 9. Magnetization versus applied field for an unannealed AuCo plating.

the saturation magnetization. This type of plot for III 8 B Unannealed is shown in Figure 10. The dashed line is the regression line fitted to the five highest field points. The Y-intercept is 143.9 μG . The ascending field measurements are given by an +, and the descending field curve points are denoted by an \square . The superposition of the two curves shows the lack of remanence and the precision of the measurements.

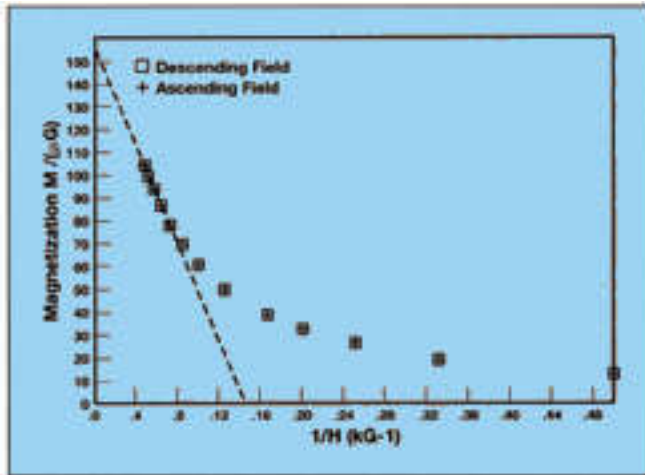


Figure 10. Plot of magnetization versus $1/H$. The method of extrapolation to infinite field is shown. Both the ascending and descending data are plotted.

An applied field of 21 kOe should not be enough to saturate the magnetic moments in this sample at room temperature if they were acting independently. The near saturation behavior can easily be explained by the presence of superparamagnetic entities of cobalt atoms in solid solution, whose magnetic properties are not completely quenched by the gold matrix. The calculation of the upper limit for the diameter of particles showing superparamagnetic behavior in the previous section gave a value of 146 Å. X-ray diffraction measurements of the effective grain size for the $\langle 111 \rangle$ direction in this sample give a value of 188 Å while the same measurement for grains with $\langle 200 \rangle$ planes parallel to the surface give a value of 130 Å. From these results it is tempting to consider the superparamagnetic entities as individual gold grains containing cobalt atoms in solution in the gold. If for some reason the cobalt atom density is greater in the interior of the grain than it is at the grain boundary, we would expect this uneven distribution of the cobalt in the grains to give rise to the type of superparamagnetic behavior that we observe.

We have shown above that individual cobalt atoms and pairs of atoms are nonmagnetic. The above behavior indicates that the magnetic interactions between nearest neighbor triplets is large enough to cause this superparamagnetic behavior in each grain. The fact that the magnetic character of the cobalt atoms depends on the distribution of neighboring solute atoms can explain the scatter in the magnetic data

for different samples as shown in Figure 6. If the distribution of cobalt atoms in the gold matrix is affected by the plating parameters, we would observe a magnetic behavior that could be different for two samples even though the average cobalt concentration were the same.

If we expand the plot in Figure 9, we see a very small hysteresis as shown in Figure 11. This hysteresis is very probably due to a small iron contamination, which is very hard to eliminate.

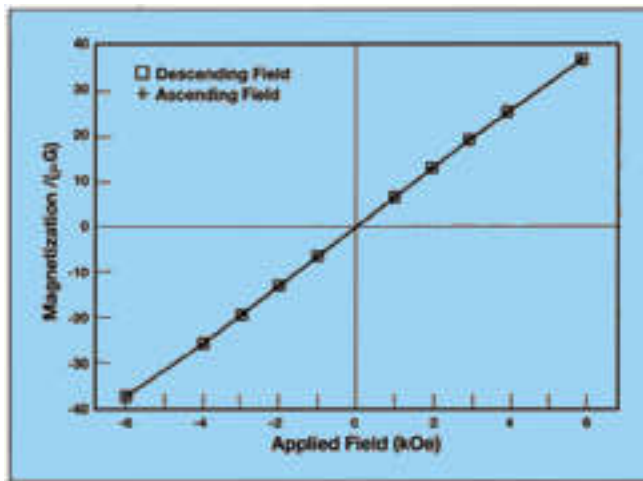


Figure 11. Magnetization versus applied field for an unannealed AuCo plating. This is an expanded plot of the data in Figure 9 to show the behavior at low fields.

Although most of the unannealed magnetization plots are qualitatively similar to the curve shown in Figure 9, 10 of the 64 unannealed platings have a magnetization curve like that shown in Figure 12. In this case we see a ferromagnetic contribution that saturates at very low fields and a diamagnetic contribution from a second phase. The easily saturated ferromagnetic contribution is again probably caused by an iron impurity in the gold bath. The hysteresis at the low field end of the plot is clear from the deviation of the ascending and descending magnetization curves. This contribution cannot be due to the dissolved metallic cobalt, since the data in Figure 9 show that the cobalt magnetization does not saturate at such low fields.

The magnetic susceptibility is equal to the slope of the magnetization versus applied field. Since the slope for this sample is negative, the magnetic susceptibility must be negative and the existence of a diamagnetic phase is evident. This cannot be due to the gold matrix, since the diamagnetic contribution from the gold has been subtracted from all the magnetization curves shown. The curves showing a diamagnetic phase are from those samples that have the smallest amounts of cobalt in the platings. If the samples are ordered in ascending values of the total cobalt content, the 10 platings with a behavior like that shown in Figure 12 occur in the 18 samples with the lowest total cobalt content.

These samples have a total cobalt content that varies from 0.150(0.5) to 0.3(1.0) wt%. Since the magnetic effect of the dissolved cobalt is proportional to the cube of the dissolved cobalt concentration, the paramagnetic behavior of samples with a low dissolved cobalt concentration should be small by comparison and the diamagnetic phase will be seen. The diamagnetic contribution will not show any cooperative effects and will be proportional to the first power of the organic cobalt content.

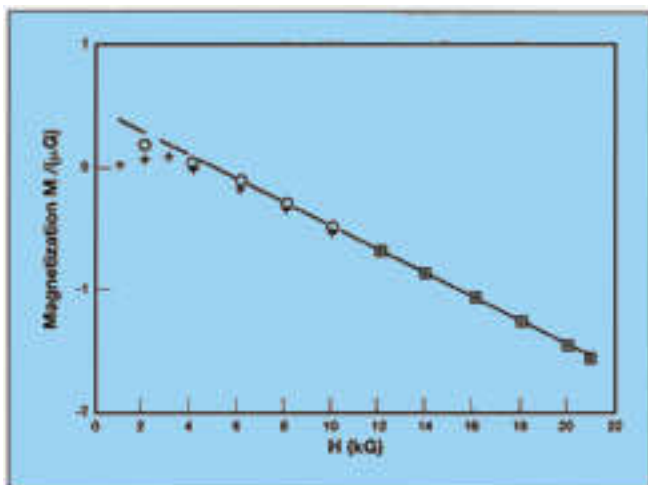


Figure 12. Magnetization versus applied field for an unannealed AuCo plating. In this sample the diamagnetic behavior is evident.

Although we see the second phase in only ten samples at room temperature, this diamagnetic phase likely exists in all the unannealed samples. In the other samples, we would expect the diamagnetic organic cobalt contribution to be masked by the larger contribution from the metallic cobalt. One method of determining this would be to analyze the magnetization curves in order to calculate the contribution of both phases to the total magnetization curve. An ideal superparamagnetic sample would show a Langevin-type behavior, but a number of factors could influence the shape of this curve. Unfortunately, the effects of a distribution in particle size, magnetocrystalline anisotropy, demagnetizing effects, and magnetostriction will all cause a flattening of the ideal Langevin curve and cannot easily be separated from the similar effect of a diamagnetic contribution.

A more accurate method of determining the diamagnetic phase concentration would be to repeat these measurements at a temperature low enough to saturate the superparamagnetic spins. In this case the contribution to the magnetization curve due to the dissolved cobalt would become constant and any further change in the magnetization with increased field would be due to the diamagnetic phase only. This is analogous to what we observe for the samples with a ferromagnetic impurity. Many susceptibility measuring instruments use an alternating field magnetometer, and one

of these could be combined with a large dc bias field in a low-temperature Dewar chamber.

We can estimate the effect of temperature on the behavior of the unannealed deposits by fitting a Langevin curve to the III 8 B Unannealed sample data. If we fit the data shown in Figure 8, using a nonlinear regression routine, we obtain the curves shown in Figure 13. The saturation magnetization of the fitted curve is 154.1 μG . This is somewhat larger than the intercept value of 143.9 μG calculated from the data shown in Figure 10. Since the M versus $1/H$ plot near small values of $1/H$ is still curving upward in Figure 10, however, a larger value of the saturation magnetization found from fitting the whole curve is understandable. The value of M/kT determined from the regression calculation is 0.4834. If we change the sample temperature from 299.66 K (26.51°C) to 77.36 K (-195.79°C), the boiling point of nitrogen, and recalculate the fitted curve, we obtain the top curve in Figure 13. As expected, the sample magnetization approaches much closer to saturation and the change in magnetization at higher applied fields is much less than we observe at room temperature. At this temperature a diamagnetic contribution to the magnetization should be easier to detect. In particular, any downward slope in the magnetization can only come from a diamagnetic phase.

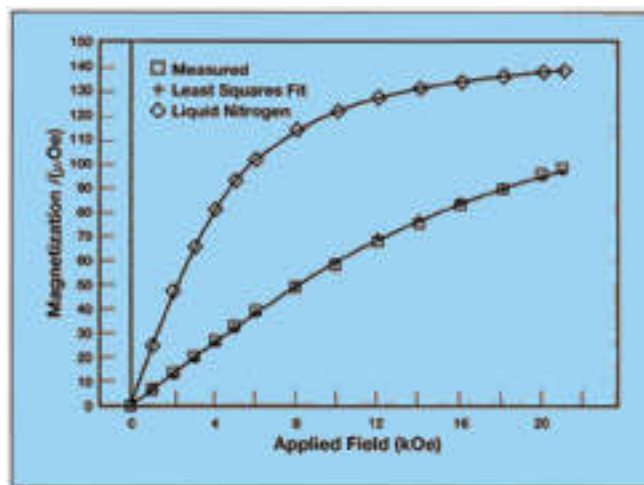


Figure 13. Least squares Langevin curve fit to measured magnetization data and extrapolation to 77 K.

Although low-temperature susceptibility measurements are preferable, we can still attempt a separation of the two phases in the unannealed state by using the data at room temperature already obtained in this study. The contribution of the metallic phase to the initial slope of the magnetization can be obtained from the annealed data, since in this state all the cobalt is dissolved in the gold matrix. If we use the data in Figure 6, we can obtain a value for the contribution of the metallic cobalt to the initial slope. The contribution of the organic cobalt to the initial slope can be obtained from the data of Sample IV 5 B Unannealed shown in Figure 12. The chemical analysis of this sample can be understood on the

basis that the cobalt in this sample is either completely metallic or completely organic, in other words, all paramagnetic or all diamagnetic. There is no chemical evidence for two phases in this sample. As the data in Figure 12 indicates, this sample is clearly diamagnetic. Since this contradicts the assumption that the sample is completely metallic, we use the alternate hypothesis that the sample contains only organic cobalt. From the cobalt content of this sample we can obtain the contribution of the diamagnetic cobalt to the initial slope. To avoid any complication from ferromagnetic impurities in the samples, the initial slope is measured for applied magnetic fields greater than 4 kOe. Since the sum of the metallic and organic cobalt must equal the measured total cobalt content, we can eliminate one of the unknown concentrations and we have an equation for each

sample slope in only one unknown. These equations were solved for each unannealed sample and the results for each of the block samples are shown in Figures 14 to 17. The results of a chemical analysis for the composition of the same samples are also shown.

A comparison of the chemical and magnetic results shows a systematic difference in the two results. The magnetic analysis indicates a smaller amount of the diamagnetic phase in most samples. This may be an artifact arising from the assumptions used in interpreting the chemical data. In these calculations, an excess of the diamagnetic cobalt in the form of $K_3[Co(CN)_6]$ is assumed. Other results, discussed below, suggest that this assumption is not substantiated for all of the samples measured.

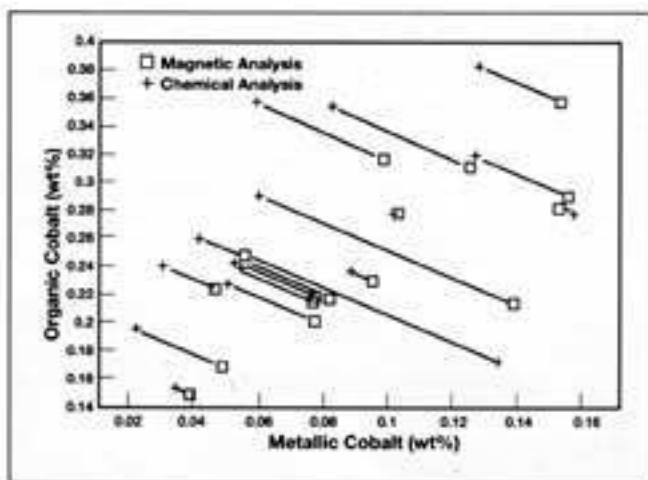


Figure 14. Organic versus metallic cobalt concentrations using magnetic susceptibility and chemical analysis. Analyses for the same sample are connected.

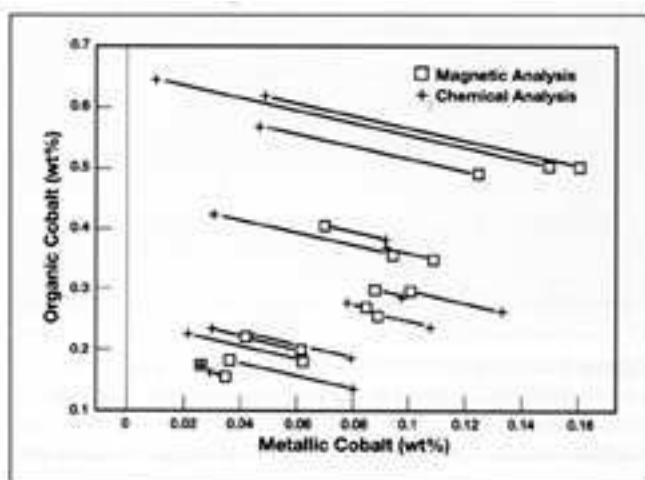


Figure 15. Organic versus metallic cobalt concentrations using magnetic susceptibility and chemical analysis. Analyses for the same sample are connected.

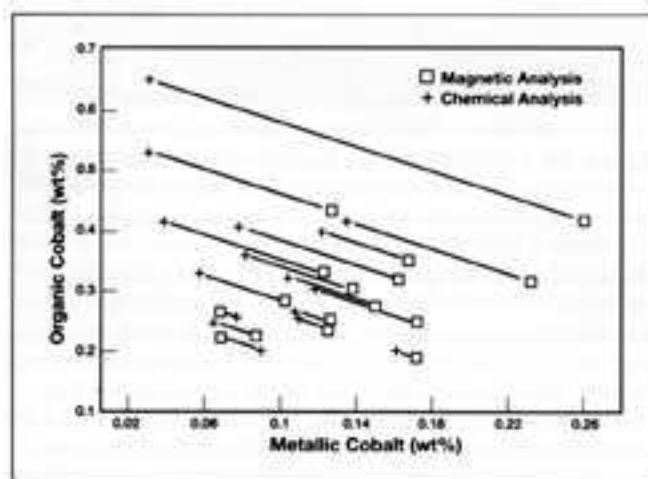


Figure 16. Organic versus metallic cobalt concentrations using magnetic susceptibility and chemical analysis. Analyses for the same sample are connected.

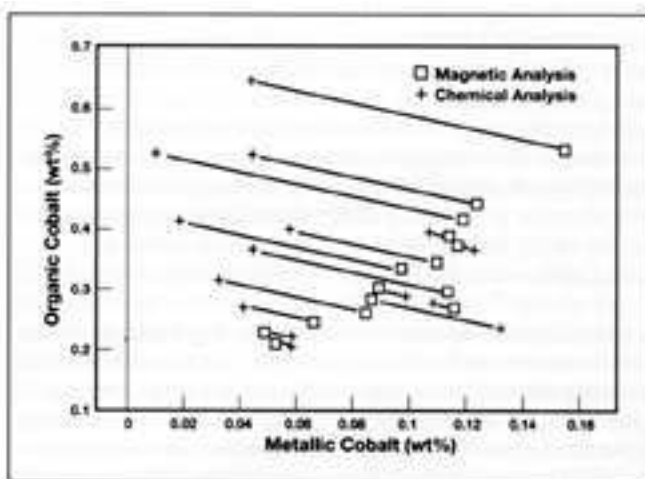


Figure 17. Organic versus metallic cobalt concentrations using magnetic susceptibility and chemical analysis. Analyses for the same sample are connected.

Since we observe that this second phase is diamagnetic, we can say something about its composition. This phase is probably the same as the numerous, small inclusions that are observed in TEM observations of cobalt-hardened gold.¹² These inclusions have a diameter of approximately 25 Å and could well be clumps of some organic cobalt-containing compound. When AuCo films are dissolved with aqua regia, a precipitate of $\text{Co}_3[\text{Co}(\text{CN})_6]_2 \cdot x\text{H}_2\text{O}$ is observed.¹³ We have prepared this compound and measured its magnetic susceptibility. Since this compound is paramagnetic, it cannot comprise the second phase. On the other hand, the compound $\text{K}_3[\text{Co}(\text{CN})_6]$ is diamagnetic, so that the presence of this compound in the plating is possible. These results agree with Mossbauer spectroscopy observations that $\text{Co}_3[\text{Co}(\text{CN})_6]_2 \cdot x\text{H}_2\text{O}$ cannot be present in the plating, whereas the $\text{Co}(\text{CN})_6^{3-}$ complex is present in the cobalt-hardened gold electrodeposit.¹⁴ Unfortunately these experiments do not say anything about the positive ions present. These results also agree with Auger spectroscopy results that are consistent with the presence of inclusions of complex potassium hexacyanocobaltate.¹⁵

Table 1 gives a list of some cobalt compounds that maybe present in the AuCo plating and their magnetic susceptibility. If we assume that the diamagnetic phase is due to $\text{K}_3[\text{Co}(\text{CN})_6]$ we can calculate the amount of this phase from the second phase cobalt content. The plot of the magnetization versus H for sample IV 5 B Unannealed is shown in Figure 12. For applied fields above 4 kOe the magnetization is a straight line with a slope of -0.0957×10^{-6} CGS-EMU. This slope is the magnetic susceptibility per gram of the gold plating.

Sample IV 5 B Unannealed has an organic cobalt content of 0.15 (0.5) wt%, from which we calculate a magnetic suscep-

Table 1. Magnetic Susceptibility

Compound	Susceptibility per mole 10^{-6} (CGS-EMU)	Susceptibility per gram 10^{-6} (CGS-EMU)	Temperature (K)	Ref.
$\text{Co}(\text{CN})_2$	+3825.0	+34.47	303	[1]
$\text{Co}(\text{CN})_2 \cdot \text{H}_2\text{O}$	+4350	+33.73	301	[21]
$\text{Co}(\text{CN})_6^{3-}$	-18700	-136.51	Amb	[21]
KCN	-37.0	-0.5682	Amb	[1]
$\text{K}_2\text{Co}(\text{CN})_6$	-60	-0.1959	Amb	[21]
$\text{K}_3[\text{Co}(\text{CN})_6]$	-132	-0.3971	Amb	[21]
$\text{K}_4[\text{Co}(\text{CN})_6]$	-103.0	-0.3099	—	[22]
$\text{K}_5[\text{Co}(\text{CN})_6]$	+54	+0.1454	290	[21]
$\text{KCo}[\text{Co}(\text{CN})_6] \cdot 2\text{H}_2\text{O}$	+11780	+33.74	293	[21]
$\text{K}_2[\text{Co}_2\text{O}_7]$	+4690	+10.098	294.2	[23]
$\text{Co}_2[\text{Co}(\text{CN})_6]_2$	+9260	+15.258	290	[24]
CoO	+4900.0	+69.08	260	[1]
Co_2O_3	+4560.0	+29.636	Amb	[1]
Co_2O_4	+7880.0	+35.054	Amb	[1]
$\text{Au}_3[\text{Co}(\text{CN})_6]$?	?	—	[7]
$\beta\text{-CoO}(\text{OH})$?	?	—	[24]
$\text{Co}(\text{CN})_3$?	?	—	[19]
$\text{H}_2[\text{Co}(\text{CN})_6]$?	?	—	[17]

tibility of -6.4×10^{-8} CGS-EMU per gram of diamagnetic cobalt. If the organic cobalt phase is potassium hexacyanocobaltate, this would mean that the susceptibility per gram of the compound must be -0.361×10^{-6} CGS-EMU. This number is quite close to the two published values for the diamagnetic susceptibility of this compound in Table 1. Since the most common impurity in a preparation of this compound would be a small amount of divalent cobalt (paramagnetic), the more negative value would seem more reliable.

A plot of the analyzed potassium content versus organic cobalt content for the 64 samples in the four blocks is shown in Figures 18–21. If the organic cobalt is indeed potassium

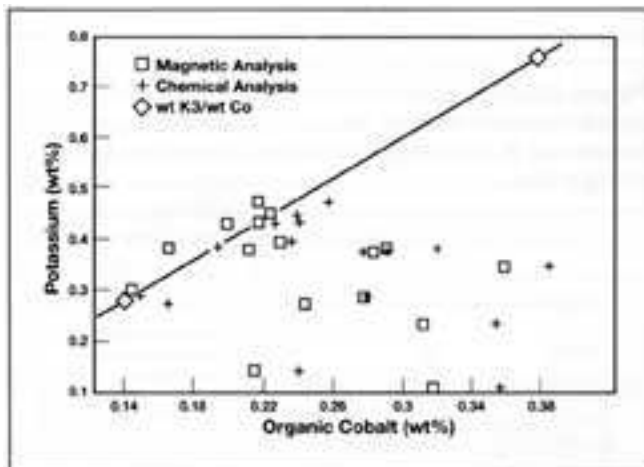


Figure 18. Potassium concentration versus organic cobalt concentration for Block 1. If the cobalt is present as $\text{K}[\text{Co}(\text{CN})_6]$, the points should lie on the straight line.

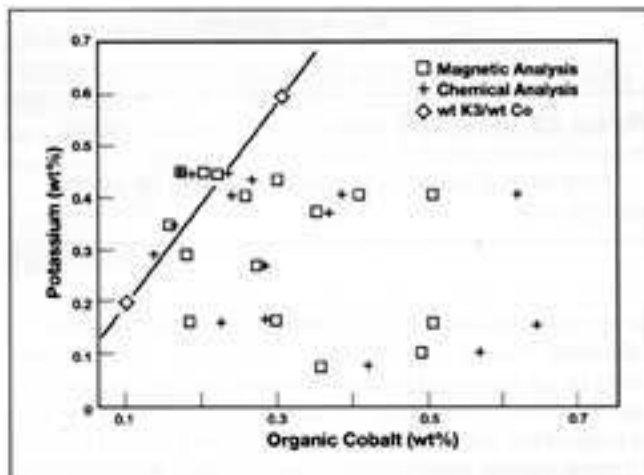


Figure 19. Potassium concentration versus organic cobalt concentration for Block II. If the cobalt is present as $\text{K}_3[\text{Co}(\text{CN})_6]$, the points should lie on the straight line.

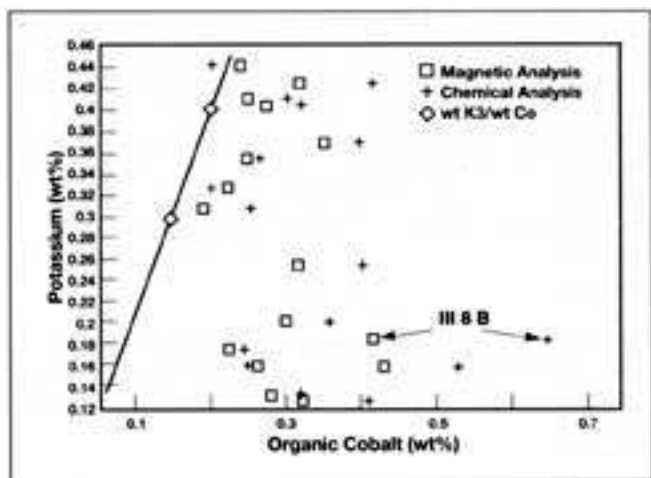


Figure 20. Potassium concentration versus organic cobalt concentration for Block III. If the cobalt is present as $K_3[Co(CN)_6]$, the points should lie on the straight line.

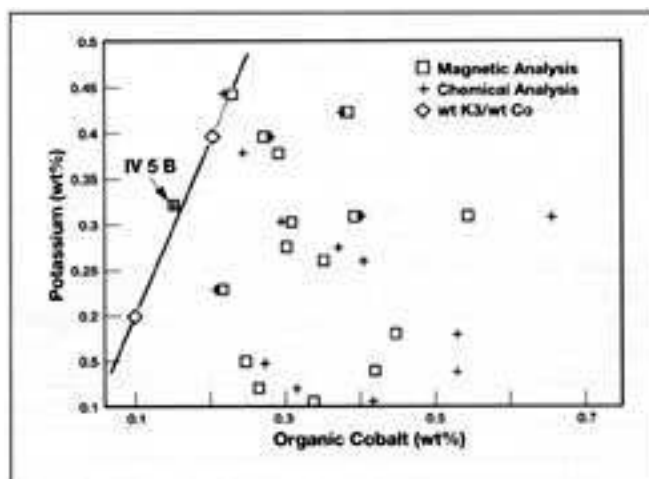


Figure 21. Potassium concentration versus organic cobalt concentration for Block IV. If the cobalt is present as $K_3[Co(CN)_6]$, the points should lie on the straight line.

hexacyanocobaltate, all of the points should fall along the calculated straight lines shown in each Figure. The fact that many of the measured points fall below the line indicates that the potassium content in many of the samples is too low to support the hypothesis. The data for Block IV in Figure 21 show that the sample IV 5 B does indeed fall close to the line predicted on the basis that the organic phase is potassium hexacyanocobaltate and confirms the susceptibility measurements discussed above. Nonetheless, it is clear that not all of the organic phase in other samples is potassium hexacyanocobaltate.

Interestingly, the data in all four blocks show that no organic cobalt phase has more than approximately three potassium atoms for each organic cobalt atom, although many have less potassium. This would suggest that the potassium and the organic cobalt are somehow connected. The samples in Block I contain smaller organic cobalt concentrations than in the other blocks, and have a greater percentage of samples lying on the all hexacyanocobaltate line (Fig. 18). The sample with the greatest cobalt content, III 8 B Unannealed shown in Figure 21, has a potassium/organic cobalt atom ratio of 0.655 for the magnetic analysis data, and 0.423 for the chemical analysis data.

These results suggest that the organic cobalt phase begins with the formation of a compound with a 3 to 1 potassium to cobalt atomic ratio, and then continues with other compounds containing less or no potassium. If this is true, then the organic phase of most samples is not composed of a single compound. On the other hand, since the magnetic behavior of the cobalt compounds resides in the cobalt-containing anion, the analysis of the magnetic data based on the assumption that all organic cobalt has the same magnetic properties may not be too far wrong.

The requirement that the second phase be diamagnetic imposes certain restrictions on the electronic structure of the cobalt in this phase. The diagrams in Figure 22 from Reference 16 show the electronic structure of the cobalt atom for various types of chemical binding. The only structure that does not have an unpaired electron, which is a requirement for diamagnetic behavior, is the octahedral covalent

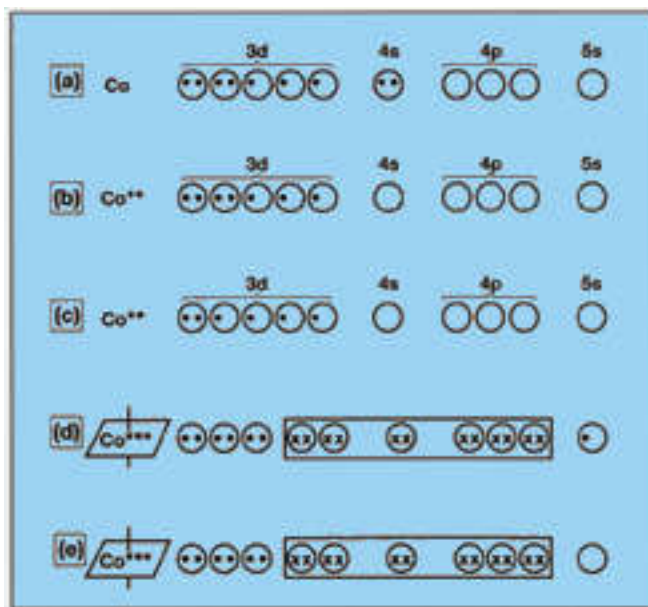


Figure 22. Effect of ionic and covalent bonding on electron distribution on atomic orbitals: **a)** metallic cobalt, **b)** Co^{++} ionic, **c)** Co^{+++} ionic, **d)** Co^{++} octahedral covalent, **e)** Co^{+++} octahedral covalent. .-ionic electron x-covalent bonded electron.

Co(III) ion (e). Since cobalt is introduced into the plating bath as Co(II) acetylacetonate (acac) and any cobalt that might be oxidized at the anode to the trivalent state should immediately precipitate as Co(acac)₃, the presence of Co(III) in the gold plating might seem surprising. One explanation is that cobalt has a great affinity for octahedral covalency with strongly electronegative groups such as (OH), (CN), etc.¹⁶ If an octahedral complex with Co(II) is formed at the cathode, this will be unstable because the one unpaired electron on the cobalt 5s orbital is easily lost to form the Co(III) covalent compound.¹⁷ We can thus understand the incorporation of Co(III) compounds into the plating at the cathode.

Although all octahedral covalent trivalent cobalt compounds are diamagnetic and possible candidates for the organic cobalt phase, we cannot reject all divalent cobalt compounds a priori. The reason for this is presumably the pairing of the odd electron by the formation of a dimer or polymer to form a diamagnetic salt. One well known example of this phenomenon is Adamson's salt K₃[Co(CN)₅]₂, which is diamagnetic. The potassium to cobalt atomic ratio in this compound is the same as the hexacyanocobaltate.

The octahedral covalent compounds of cobalt can form quite complex structures. One proposed structure for Co(CN)₂ is shown in Figure 23.18. In this structure the framework consists of Co(CN)₃ units. To preserve stoichiometry, a Co(II) atom must be present in the interior of every other cube. If the cobalt atoms in the framework are Co(III), the framework is now stoichiometric and no other cations are necessary. This new compound would be compatible with

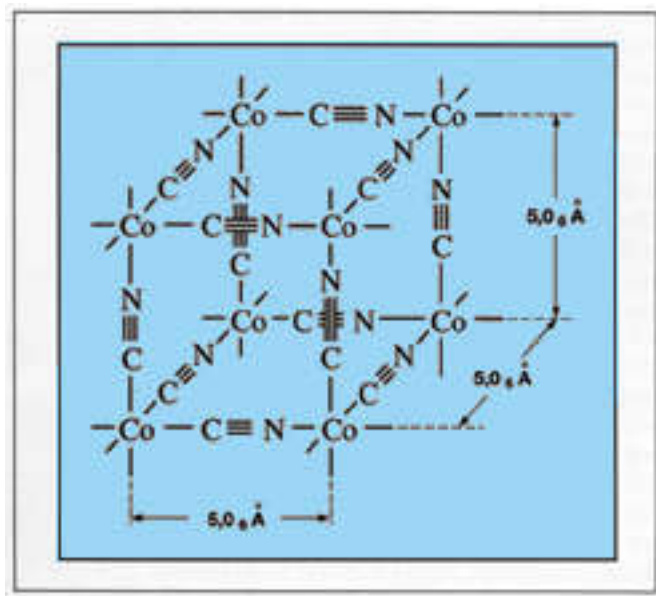


Figure 23. Three dimensional cubic structure proposed for the compound Co(CN)₂. The framework consists of Co(CN)₃ units. This structure is stoichiometric for Co+++ ions.

the results of both Mossbauer spectrometry and the present magnetic measurements. Although the compound Co(CN)₃ is reported to exist, one author reports that it is paramagnetic, which is hard to understand.¹⁹ It may be that the preparations still contain some divalent cobalt as an impurity. At any rate, I am not aware of any published data on the structure of Co(CN)₃.

CONCLUSIONS

The structure of the metallic cobalt phase seems unambiguous. Unfortunately, it seems impossible to be more specific about the structure of our organic phase in view of the complicated structures that can be imagined for these cobalt compounds, especially if some of the cyanide units were replaced with OH units.

The properties of the metallic and the organic phases in the gold plating play an important role in the mechanical behavior of these platings.¹ Since we cannot be sure of the exact form of the diamagnetic compound that is present in the alloy, we cannot be more specific. It may be that x-ray photoelectron spectroscopy will determine the structure of the diamagnetic phase in more detail. This technique is frequently used to distinguish paramagnetic and diamagnetic phases in transition metal samples.²⁰

These results show that the study of the magnetic properties of AuCo platings has been very helpful in analyzing their structure. Magnetic force measurements are especially useful in separating the effects of the metallic and organic phases in the electroplate with a minimum of wet chemistry techniques. It would be expected that additional measurements of the magnetic properties of diamagnetic cobalt compounds would lead to more information on the structure of the organic cobalt phase.

ACKNOWLEDGMENTS

I would like to thank Marsha Lower for some of the sample preparation, Sally Keister for the sample preparations and the sharing of her analysis results, and Glenn Staudt for many helpful discussions.

REFERENCES

1. R. De Doncker and J. Vanhumbecck, *Trans. Inst. Met. Finishing* 63(2), 59 (1985).
2. T.B. Massalski, ed., *Binary Alloy Phase Diagrams* (ASM, Metals Park, 1986), p. 249.
3. C-W. Chen, *Magnetism and Metallurgy of Soft Magnetic Materials* (Dover, New York, 1986), p. 100.
4. R.C. Weast, ed., *CRC Handbook of Chemistry and Physics*, 66th ed. (CRC Press, Boca Raton, 1985), p. E-117.

5. C.P. Bean and J.D. Livingston, *J. Appl. Phys.* **30**(4), 120S (1959).
6. C-W. Chen, p. 69.
7. C.P. Bean, *J. Appl. Phys.* **26** (11), 1381 (1955).
8. D. Martin, *Magnetism in Solids* (M.I.T. Press, Cambridge, 1967), p. 19.
9. C-W. Chen, p. 38.
10. E. Boucai et al., *Phys. Rev.* **B3** (11), 3834 (1971).
11. M.W. Daybell and W.A. Street, *Rev. Mod. Phys.* **40**(2), 380 (1968).
12. S. Nakahara, *J. Electrochem. Soc.* **136**(2), 451 (1989).
13. E.T. Eisenmann, *J. Electrochem. Soc.* **124**, 1957 (1977).
14. R.L. Cohen et al., *J. Electrochem. Soc.* **126**(9), 1608 (1979).
15. A.J. Bentley et al., *Nut. Instr. Meth. Phys. Res.* **218**, 555 (1983).
16. L. Pauling, *The Nature of the Chemical Bond*, 3rd ed. (Cornell Univ. Press, Ithaca, 1960), p. 338.
17. L. Pauling, p. 149.
18. A. Weiss and W. Rothenstein, *Agnew. Chem. Intemat. Ed.* **2**(7), 396 (1963).
19. P.C. Selwood, *Magnetochemistry* (Interscience, New York, 1943), p. 173.
20. T.A. Carlson, *Photoelectron and Auger Spectroscopy* (Plenum Press, New York, 1975), p.231.
21. D.K. Kalani, *Laboratory Practice* **17**(6),691 (1968).
22. C.R. Kanekar and S.V. Nipankar, *Jour. Indian Chem, SOC.* **43**(6), 397(1966).
23. M. Jansen and R. Hoppe, *Z. anorg. allg. Chem.* **409**, 152 (1974).
24. H. Leidheiser et al., *J. Electrochem. Soc.* **126**(3), 391 (1979).

David Kahn is a Senior Member of the Technical Staff in the Metal Processing Technology Group at AMP Incorporated in Harrisburg, Pennsylvania.

Dr. Kahn received a B.S. in engineering physics from the University of Illinois and a Ph.D. in physics from the University of Chicago. He was subsequently employed at the Lewis Laboratory of NASA and the Martin Marietta Research Laboratory. Since joining AMP, he has worked in the areas of transition metal compounds, electrical contact oxidation and stress relaxation, the characterization of metal platings, and multivariate analysis of plating systems.